

High Pressure Research on Materials

2. Experimental Techniques to Study the Behaviour of Materials under High Pressure

P Ch Sahu and N V Chandra Shekar

In this part¹ of the article, various experimental techniques for investigating materials under high pressure are discussed. The effect of pressure on the behaviour of materials is discussed with suitable examples.

1. Introduction

Before the introduction of diamond anvil cell (DAC) in the early seventies, conventional high pressure generating devices like the piston-cylinder apparatus, Bridgman opposed anvil devices, and multi-anvil devices, along with experimental techniques like electrical resistivity measurement, thermoelectric power measurement, and X-ray diffraction were adopted to study materials under high pressure. The pressure capability was also limited to about few tens of giga Pascals (GPa). However, after the introduction of DAC, the situation completely changed. Not only was the pressure generating capability enhanced to several hundreds of giga Pascals, but also advanced experimental spectroscopic techniques like X-ray, Raman, Brillouin, IR, luminescence, optical reflectivity, positron and Mössbauer, were introduced to study materials under high pressure. It is also possible to focus high power IR lasers onto the pressurized samples inside the DAC to raise the sample temperatures to ~ 5000 K, thereby simulating the conditions in the earth and planetary interiors. This additional capability of simultaneously applying high pressure and high temperature in a DAC underlines the spectacular research tool called the Laser Heated Diamond Anvil Cell (LHDAC). Further, with the development of synchrotron radiation sources, which provide very high brilliance X-ray, ultra violet-visible photon beams, it is possible to investigate matter *in-situ* at such extreme



P Ch Sahu (left) is at the Materials Science Division of Indira Gandhi Centre for Atomic Research, Kalpakkam. He is a specialist in the field of high pressure science and is presently heading this activity at his institute.

N V Chandra Shekar (right) is a Senior Scientist at the Materials Science Division of Indira Gandhi Centre for Atomic Research, Kalpakkam. His primary research areas are in high pressure phase transitions and in synthesis and study of novel materials under extreme pressure and temperature conditions.

¹ Part 1. Production and Measurement of High Pressures in the Laboratory, *Resonance*, Vol.12, No.6, pp.10–23, June 2007.



The effect of pressure on materials is very dramatic. It not only brings the constituent atoms and molecules closer to form denser and compact phases, but also causes drastic changes in their electronic structure, which in turn profoundly alters the macroscopic properties: density, colour, opacity, ductility, electrical conductivity, etc.

pressure and temperature conditions very rapidly (shorter exposure times due to high photon flux).

The effect of pressure on materials is very dramatic. It not only brings the constituent atoms and molecules closer to form denser and compact phases, but also causes drastic changes in their electronic structure, which in turn profoundly alters the macroscopic properties: density, colour, opacity, ductility, electrical conductivity, etc. The effect of pressure on materials is much more pronounced compared to that of temperature. For example, the maximum volume change in a solid before it melts is $\sim 10\%$, whereas a moderate pressure of ~ 100 GPa can change the volume of a solid by more than 70% .

In this part, various experimental techniques that are being used in conjunction with various high pressure devices are described. The effect of pressure on the physical properties of materials is presented with suitable illustrative examples. Exciting new developments in this field form the proceedings of the AIRAPT conference (see *Box 1* for more details) held every two years.

2. High Pressure Experimental Techniques

In Part 1, we classified pressure generating devices as piston-cylinder type apparatus and opposed anvil type apparatus. The state-of-the-art high pressure generating device, the DAC, falls under the latter category. In the following, we describe the experimental techniques that can be incorporated with each type of apparatus.

2.1 With Piston-Cylinder Type Apparatus

Piston-cylinder type apparatus are useful for measuring the compressibility of fluids, high pressure-high temperature electrical resistivity, and thermoelectric power of materials under hydrostatic pressure environment, using a suitable liquid as the pressure transmitting medium. A methanol-ethanol mixture or silicone oil is used for hydrostatic pressure experiments up to ~ 10 GPa. For resistivity and thermoelectric power measurements, a

Key words

High pressure, electrical resistivity, X-ray diffraction, phase transition.



Box 1. AIRAPT History

International Conference on High Pressure Science and Technology (AIRAPT) is held every two years, and attracts hundreds of high pressure scientists, engineers and industrialists all over the world. AIRAPT grew from the Gordon Research Conference on Research at High Pressures (GRCHP), the first one of which was held in 1955. The Gordon conference incorporates research from the international community. However, the GRCHP is always held in USA and limited in size. In the year 1962 at GRCHP, O Anderson, Prof at Columbia University, jumped up to the speaker's rostrum and said to the conferees, "Why don't you organize a Gordon Conference in Europe?" There was general agreement. Since the name Gordon Conference is protected, a new name was needed. The founders, BVodar (France), H LI Pugh (UK), L Deffet (Belgium), C J M Roijmans (The Netherlands), J Osugi (Japan), L F Vereschagin (USSR) and E U Franck (Germany) decided to establish a new international organization dedicated to high pressure research. Prof Deffet suggested the official name. In 1991, it was held in Bangalore, organized by Prof A K Singh then in National Aeronautics Laboratory. The next AIRAPT will be held at Catania, Sicily, Italy during September 2007.

In AIRAPT, the Bridgman Award is conferred on a distinguished Scientist for outstanding contributions to the field of high pressure science and technology. This was named in honour of P W Bridgman (1882-1961), the father of 'Modern High Pressure Research' (See Box 1 in Part 1 of this article). The first Bridgman Award was won by Prof H Drickhamer in 1977 and by S M Stishov in the year 2005.

teflon cell is used to contain the sample and the pressure transmitting liquid inside the high pressure chamber. Thin metal wires are used for making electrical contact to the sample. *Figure 1* shows a typical arrangement for measuring the pressure dependence of electrical resistance and thermoelectric power of materials using the piston-cylinder apparatus. Direct volume changes of solid and liquid materials can also be measured with this device.

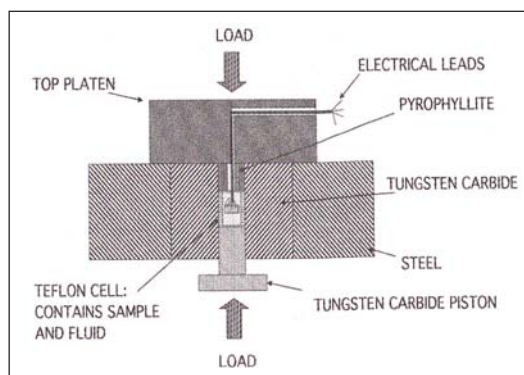


Figure 1. Schematic diagram of a piston-cylinder apparatus with teflon cell for measuring electrical resistivity of materials under high pressure and temperature.

2.2 With Opposed Anvil Type Apparatus

With opposed anvil type of apparatus, the most commonly used experimental techniques are electrical resistivity, thermoelectric power and X-ray diffraction (XRD). *Figure 2* shows the schematic arrangement for studying the pressure dependence of electrical resistivity of materials developed at IGCAR. A four probe method is used to measure the electrical resistivity as a function of pressure (up to 10 GPa) and temperature (up to 1500 K).

X-ray diffraction studies can be carried out either in the energy dispersive (EDXD) or angle dispersive (ADXD) mode. Both are based on Bragg's law:

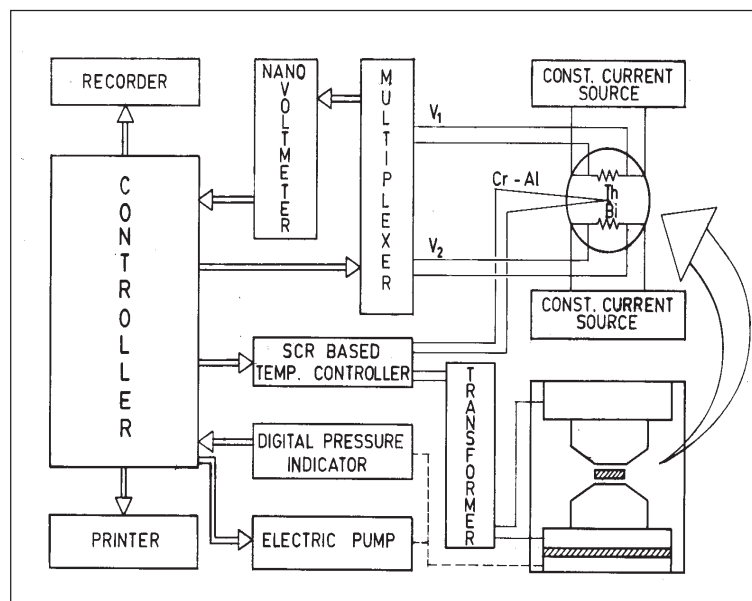
$$2d_{hkl} \sin\theta_{hkl} = \lambda_0 \quad \text{for ADXD} \quad (1)$$

and

$$2d_{hkl} \sin\theta_0 = hc/E_{hkl} \quad \text{for EDXD.} \quad (2)$$

Here, h is the Planck's constant and c is the velocity of light. In ADXD, a monochromatic X-ray beam of wavelength λ_0 is incident on the sample (as shown in *Figure 3a*) and the diffracted Bragg peaks are detected with a suitable detector as a function of θ . In EDXD, a polychromatic (white) X-ray beam is incident on

Figure 2. Experimental set up for resistivity measurement at high pressure and temperature.



the sample (as shown in *Figure 3b*) and the diffracted beam is collected at a fixed angle θ_0 by using a solid state detector (SSD). The diffracted peaks are energy analysed using a multi-channel analyser. In ADXD, the measured diffracted intensity is plotted as a function of θ or 2θ in degrees, whereas in EDXD, the intensity is plotted as a function of energy (E) in keV. Both techniques have their relative merits and demerits. For example, in EDXD, there are no moving parts as the diffracted beam is collected at a fixed angle with the SSD, but the resolution of the diffraction data is poor due to the inherent poor energy resolution of the SSD. In ADXD, either a PSD or imaging plate is used for detecting the diffracted X-rays. The resolution of ADXD data is

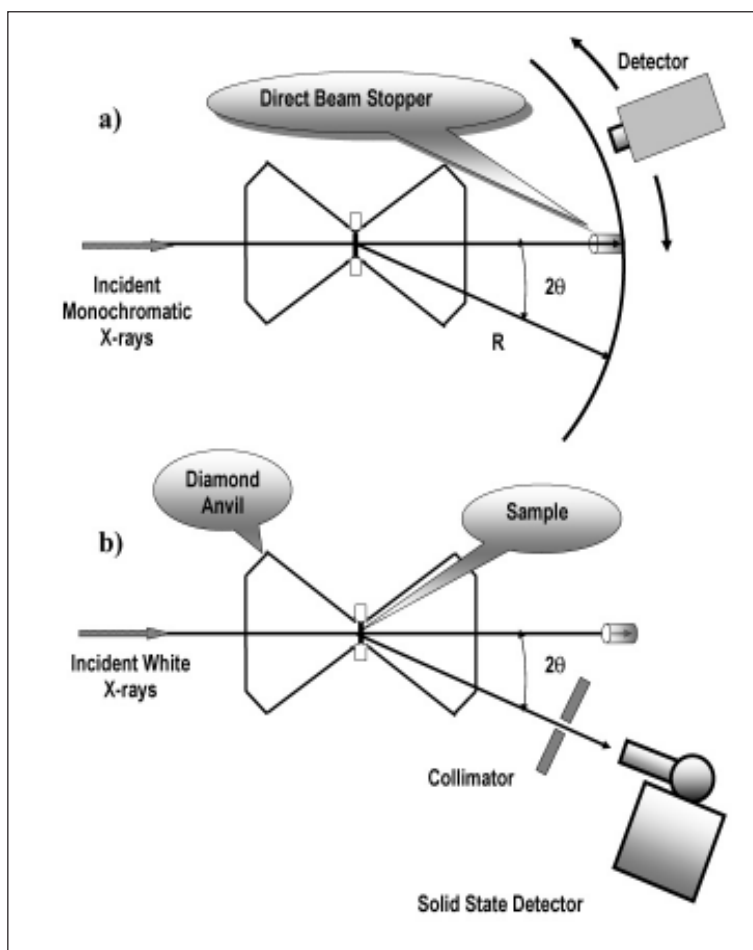


Figure 3. X-ray diffraction in (a) angle dispersive (ADX) and (b) energy dispersive (EDXD) geometry.

The incident X-ray beam can either be passed along the axis of the cell through the anvils or perpendicular to the axis. The first configuration is called *axial geometry*, and the second one *transverse geometry*.

about one order of magnitude better than that of EDXD. Recently, X-ray CCDs are being used for fast collection of ADXD data. Generally, a rotating anode X-ray generator with Mo target is used as the X-ray source. Nowadays, synchrotron radiation sources are being used for fast and efficient collection of high pressure X-ray data.

The incident X-ray beam can either be passed along the axis of the cell through the anvils or perpendicular to the axis. The first configuration is called *axial geometry*, and the second one *transverse geometry*. In axial geometry (*Figure 3*), the anvils have to be made of low Z materials like boron carbide (B_4C). In transverse geometry, the gaskets are made of X-ray transparent materials like B or Be. In this geometry, the X-ray beam traverses along the entire dimension of the sample spanning the full pressure gradient across it. In axial geometry, the pressure gradient across the sample is avoided by using a fine collimated beam (beam diameter $\sim 50\text{--}100\ \mu\text{m}$).

2.3 With Diamond Anvil Cell

With DAC, it is possible to carry out a variety of experiments such as X-ray diffraction, X-ray spectroscopy, Raman, Brillouin, IR and luminescence spectroscopy, optical reflectivity, positron and Mössbauer spectroscopy, and NMR,. This is possible due to the transparency of diamond to almost the entire electromagnetic spectrum. *Figure 4a* shows the schematic of the high pressure ADXD facility developed at IGCAR. *Figure 4b* shows the photograph of the same. The incident X-ray beam is obtained from an 18 kW rotating anode X-ray source with four windows. Another popular high pressure technique with DAC is the Laser Raman Spectroscopy (LRS). The lattice properties of solids can be probed by LRS and can be used to study the vibrations of the optical lattice modes under pressure. *Figure 5* illustrates the schematic arrangement for LRS: an incident laser beam is focused on the sample and the scattered beam is collected and focused onto a spectrometer for detection. The mechanism of LRS is as follows: An incident photon (E_i, k_i) impinging on the



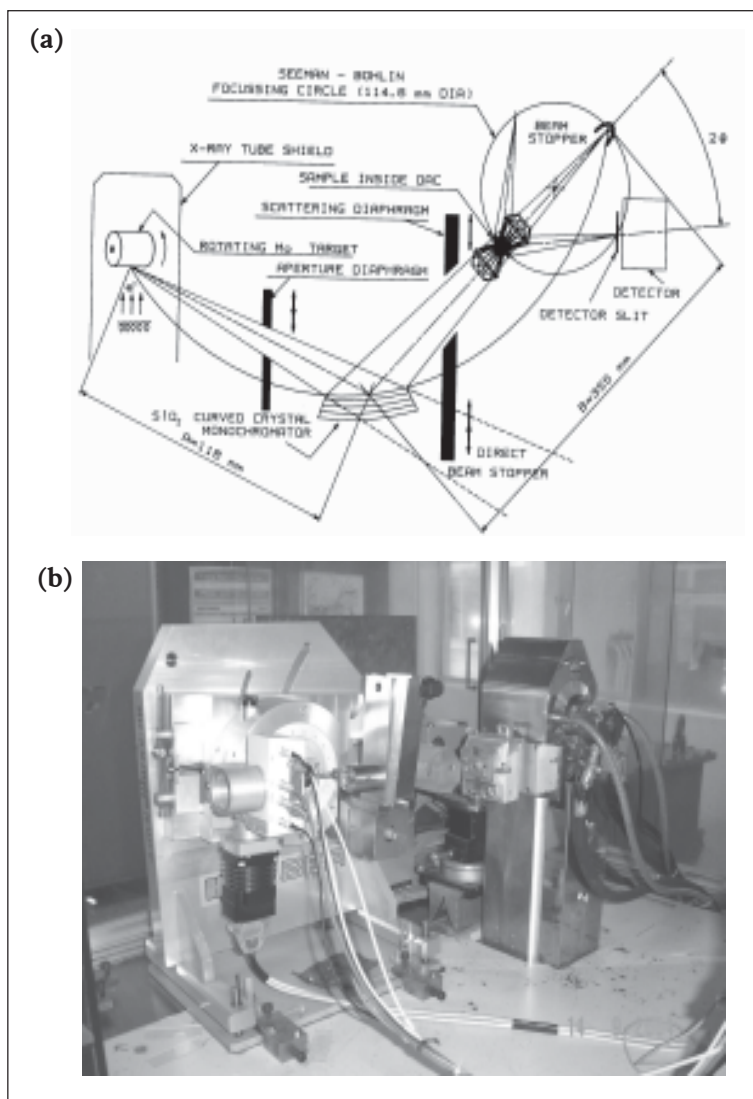


Figure 4. (a) Schematic and (b) photograph of the high pressure powder ADXD system using a DAC in Guinier geometry.

sample annihilates or creates a phonon (E_L, q); and the scattered photon (E_s, k_s) satisfies the energy $E_s = E_i \pm E_L$ and momentum $k_s = k_i \pm I$ conservation.

Measurement of resistivity and thermoelectric power using DAC is somewhat difficult, but ingenious methods have been developed. Nowadays, a fully fabricated multitasking designer diamond anvil containing two or more integrated sensors for electrical measurements, electrical heating and magnetic



Figure 5. Schematic arrangement for high pressure Laser Raman spectroscopy using DAC.

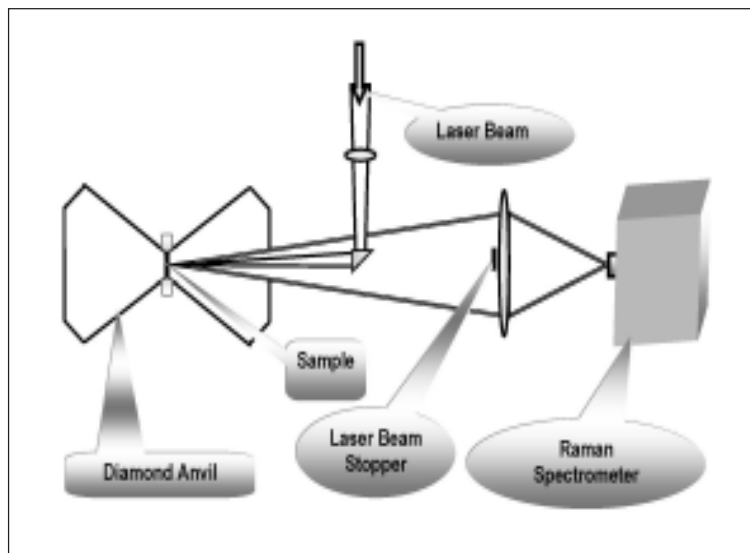
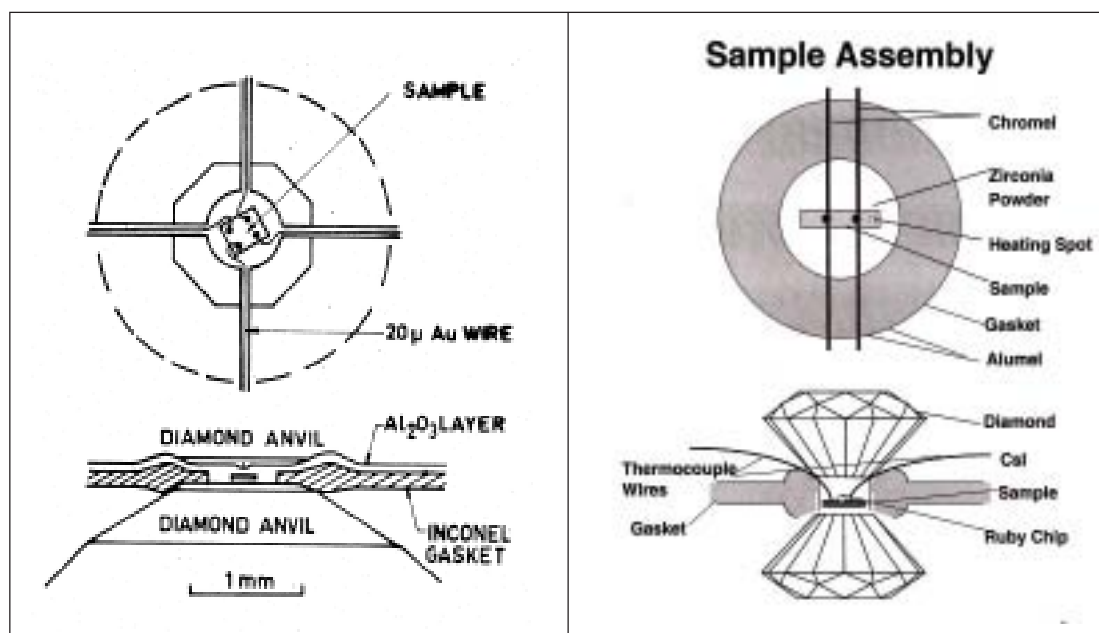


Figure 6 (left). A typical sample assembly for electrical resistivity measurement in a DAC.

Figure 7 (right). Sample assembly for thermoelectric power measurements in a DAC.

susceptibility measurements are being developed in advanced laboratories by CVD technique. *Figure 6* shows a typical sample assembly for resistivity measurement and *Figure 7* shows a sample assembly for thermoelectric power measurement using laser heating in a DAC.



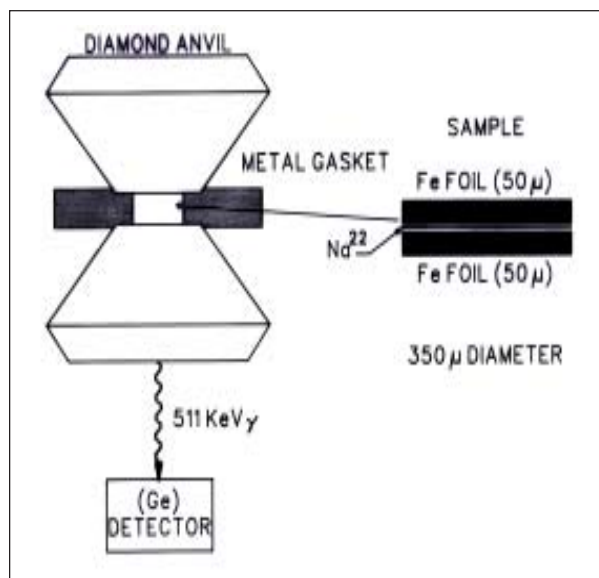


Figure 8. Experimental configuration for positron annihilation studies under high pressure using a DAC.

Figure 8 shows the schematic arrangement for carrying out positron annihilation studies under high pressure using a DAC. The Fe sample in the form of two foils, sandwiches a positron emitting Na^{22} source. For Mössbauer spectroscopy using DAC, the Mössbauer source can be positioned closer to one diamond and the γ -ray detector at the other diamond.

3. Effect of Pressure on Condensed Matter

The effect of pressure on materials can be broadly classified into two categories: lattice compression and electronic structure change. However, these two effects are not totally independent but are coupled.

3.1 Lattice Effect

These include decrease in interatomic distances or increase in density leading to changes in the phonon spectra, increase in the free energy (G) and the associated phase transitions stabilizing compact structures characterized by significant changes in the physical properties.

As the atoms are brought closer by the application of pressure, the lattice becomes stiffer and more incompressible since the atoms

The effect of pressure on materials can be broadly classified into two categories: lattice compression and electronic structure change.



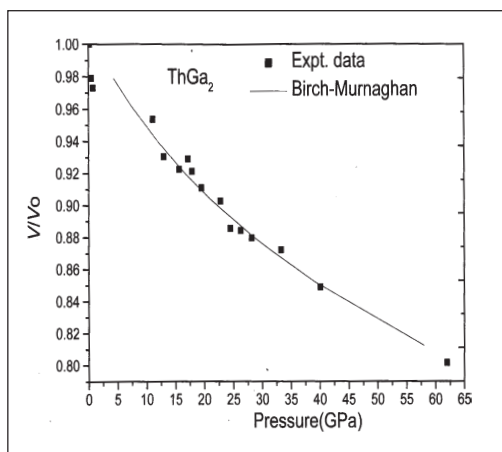


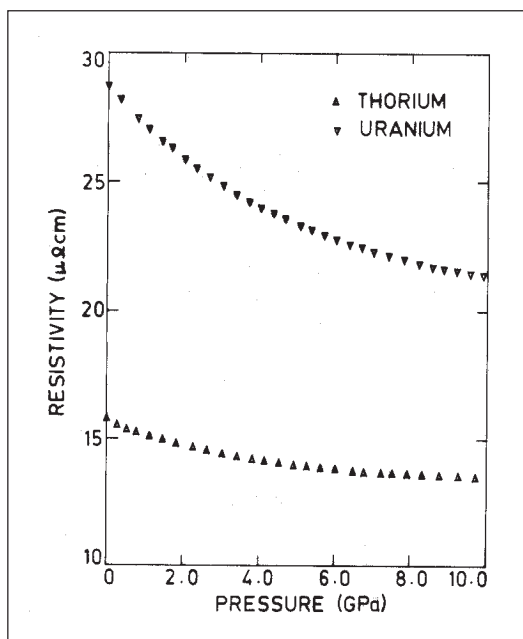
Figure 9. P–V relation for ThGa₂ up to ~60 GPa.

electrical resistivity ρ of a simple metal is given by the expression

$$\rho = m/ne^2\tau. \tag{3}$$

Here, n is the number of free electrons per unit volume, e is the electronic charge, τ is the relaxation time and m is the effective mass of the electrons. In this expression, m and e are insensitive to pressure, whereas n and τ increase with pressure. The number of free electrons (N) remains unchanged, but the volume (V)

Figure 10. Pressure dependence of θ for Th and U.

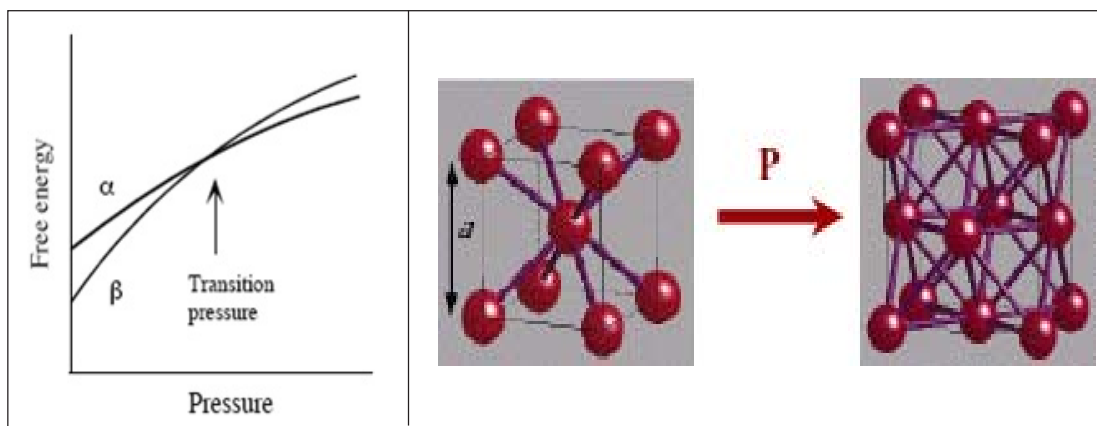


decreases with pressure leading to increase in $n = N/V$. Similarly, τ which is proportional to θ_D , also increases with pressure. Hence in general, ρ of metals should decrease with pressure. The pressure dependence of ρ for Th and U measured at IGCAR are shown in Figure 10. Similarly, the lattice specific heat C_L , which is proportional to $1/\theta_D^3$, is expected to decrease with pressure.

The free energy of a solid is given by the expression

$$G = E - TS + PV \tag{4}$$

A minimum G stabilizes a crystal structure at ambient conditions. But the free energy of a



solid increases with pressure, and at higher pressures, the minimum free energy criterion for the parent structure may not be satisfied. In that case, the system may undergo a phase transition to a new structure which satisfies the minimum free energy criterion. *Figure 11* shows the free energies for two phases α and β as a function of pressure. To start with, the β phase with lower free energy is the stable phase. With pressure, the free energies of both phases increase, but at different rates. The free energy of the β phase increases faster compared to that of the α phase, and eventually it overtakes the latter at the transition pressure. At this point, the system may undergo a structural transition to the α phase to satisfy the minimum free energy condition. For example, the alkali metals (Na, K, Rb, Cs) are found in the BCC² phase at atmospheric pressure; but all these transform to the FCC³ phase at various pressures (*Figure 12*). We also know the simple phase diagram of water having three phases: solid (ice), liquid and vapour. It is surprising to note that solid ice under pressure exhibits about a dozen phases (*Figure.13*). Such transitions are generally first order in nature and are associated with volume discontinuities. *Figure 14* shows the high pressure X-ray diffraction (HPXRD) pattern of ThAl_2 obtained at IGCAR, which undergoes structural transitions from the parent hexagonal phase to the orthorhombic phase at about 12 GPa, and from orthorhombic to the tetragonal phase at 22 GPa.

Figure 11 (left). Schematic diagram showing the increase of free energy with pressure for two typical α and β phases.

Figure 12 (right). BCC to FCC transition in alkali metals under high pressure.

² BCC: Body Centred Cubic crystal structure in which eight atoms occupy the eight corners and one atom at the body centre position of the cube.

³ FCC: Face Centred Cubic crystal structure in which eight atoms occupy the eight corners and six atoms at the centres of six faces of the cube.



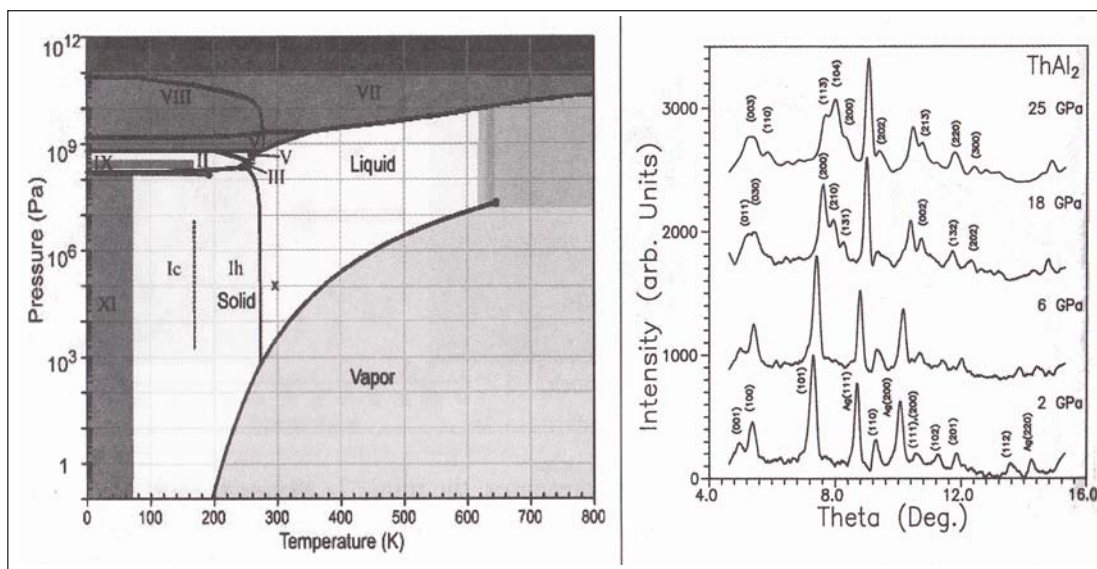


Figure 13 (left). The phase diagram of water.

Reprinted with permission from Prof. Martin Chaplin from his article "Water Structure and Science" appearing in the website: www.lsbu.ac.uk/water/.

Figure 14 (right). High pressure XRD patterns of ThAl₂. It transforms from the parent hexagonal to the orthorhombic phase at 12 GPa and from orthorhombic to the tetragonal phase at 22 GPa. The crystal structures at various pressures are as following: hexagonal (2 and 6 GPa), orthorhombic (18 GPa) and tetragonal (25 GPa).

3.2 Electronic Effects

As the interatomic distance decreases, the overlap of outer electronic orbitals in a solid increases. This leads to the following three principal effects in its electronic structure:

- Broadening of the electronic energy bands (i.e., increase in the energy band widths).
- Shifting of the energy bands with respect to the Fermi energy E_F , and
- Shifting of the Fermi level itself to higher values.

The energy difference between the top and bottom of an energy band is defined as the bandwidth W . It increases with pressure, but the magnitude of increase depends on the orbital quantum number l by the relation:

$$W(P) = W(0) [V(P)/V(0)]^{-(2l+1)/3}. \quad (5)$$

Thus energy bands with higher l (such as d ($l=2$) and f ($l=3$)) expand more compared to that of lower l (such as s ($l=0$) and p ($l=1$)).

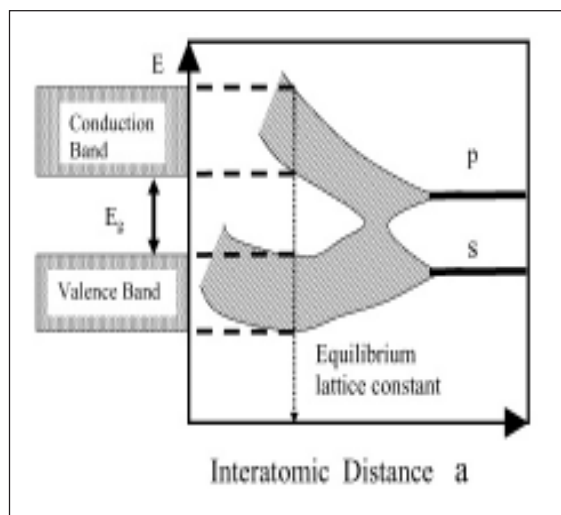


Figure 15. Sharp energy levels widening into bands, shifting and overlapping of energy bands with decreasing interatomic distance can be seen. Here, s and p denote the electron states.

Also, it is known that the kinetic energy compositions of one electron valence eigenvalues are different for different l . For example in actinide elements, the $7s$ orbitals with 6 radial nodes (number of nodes = $n - l - 1$) have more kinetic energy than the $6d$ orbitals with only 3 nodes. Their energies are nevertheless comparable at ambient conditions due to the off-setting potential energy contributions. Given the volume scaling of kinetic ($V^{-2/3}$) and potential ($V^{-1/3}$) energies, compression with pressure upsets this balance, so that the sp of the valence band tends to rise up relative to the df components. (The volume dependences of the kinetic and potential energies follow from their k dependence: kinetic energy $\rightarrow k^2$ and potential energy $\rightarrow k$). The Fermi energy E_F (which also scales as $V^{-2/3}$) shifts up to maintain the same fraction of filled states as the Brillouin zone⁴ expands due to contraction of the lattice. Figure 15 shows the sharp energy levels widening into bands, and shifting and overlapping of energy bands with decreasing interatomic distance.

All these electronic effects lead to interesting changes in the physical and chemical properties. For instance, closing of energy gaps leads to metal–insulator transitions, shift in energy bands leads to interband electron and valence transitions, change in the topology of the Fermi surface leads to Lifshitz type transitions⁵.

⁴ Brillouin zone: A Brillouin zone is defined as a Wigner-Seitz cell in the reciprocal lattice. The first Brillouin zone is the smallest volume entirely enclosed by planes that are perpendicular bisectors of the reciprocal lattice vectors drawn from the origin to the nearest reciprocal lattice points.

⁵ Lifshitz type transition: The Lifshitz or the *electronic topological transition* (ETT) occurs when a singularity in the electronic density of states arises at the Fermi level. This can happen due to the distortion of the electronic band structure as a function of pressure or temperature and results in the distortion of the Fermi surface.



Figure 16 (left). Schematic energy band diagram of an insulator/semiconductor showing the I-M transition.

Figure 17 (right). A rectangular shaped SmS sample under high pressure inside a DAC. (Courtesy: A Jayaraman)

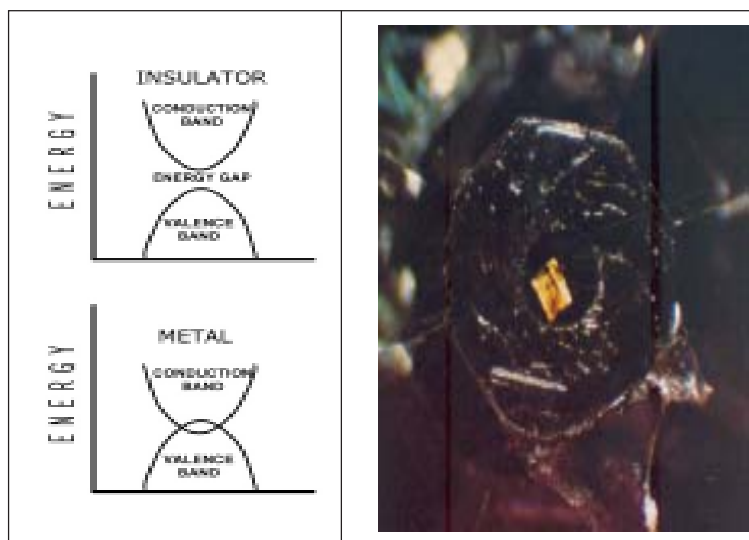


Figure 16 shows the schematic energy band diagram of a semiconductor/insulator at ambient pressure and also at a higher pressure where the bands overlap giving rise to insulator \rightarrow metal transitions. Well known examples are C, Si, Ge, and I. Even diamond, which is an electrical insulator at atmospheric pressure, is expected to become a metal at ~ 900 GPa. It is also expected that at tera Pascals of pressure the entire periodic table will consist of only metals. Also hydrogen, a molecular gas at ambient pressure, is expected to become a metallic superconductor at extreme pressures. This has yet to be demonstrated and haunts experimentalists as the most interesting and difficult problem. Spectacular changes in physical properties also occur across the insulator \rightarrow metal transitions. For example, SmS, which is a dull black semiconductor at atmospheric pressure, glitters like gold (as shown in Figure 17) when it transforms into a metal at ~ 7 GPa. It reverts back to its original black colour on releasing the pressure. Interband transfer of electrons at E_F ($s-d$ transfer) leading to significant changes in physical properties are seen in transition metals (including rare-earths and actinides) and alkali metals. As discussed earlier, the ρ of a metal should decrease with pressure in general. However the ρ of Am metal increases with pressure (Figure 18). This is due to the transfer of conduction sp electrons to the more localized df band, in which the electrons are heavier



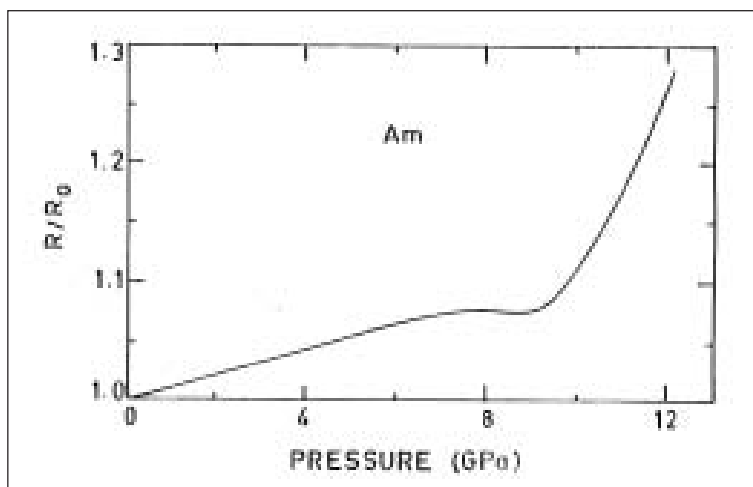


Figure 18. Electrical resistivity vs pressure for Am metal.

(This figure was published in *Journal of Physics and Chemistry of Solids*, Vol.29, D R Stephens, H D Stromberg and E M Liley, Phase Diagram, Compressibility and Resistance of Americium as a Function of Pressure, pp.815–821, Copyright Elsevier, 1968).

and more immobile. The change in topology of the Fermi surface gives rise to Lifshitz type (electronic topological transitions or ETT) transitions, associated with changes in their bulk properties (specific heat, \tilde{n} , bulk modulus, etc.).

The combined pressure-induced lattice and electronic effects manifest as dramatic changes in the superconducting and magnetic properties. For instance, Fe which is a ferromagnet with BCC structure at atmospheric pressure, loses its magnetism at ~ 12 GPa associated with a transition to HCP structure. Further, it becomes a superconductor in the pressure range 15–30 GPa, above which it again becomes a normal conductor. *Figure 19* shows the phase diagram of Fe.

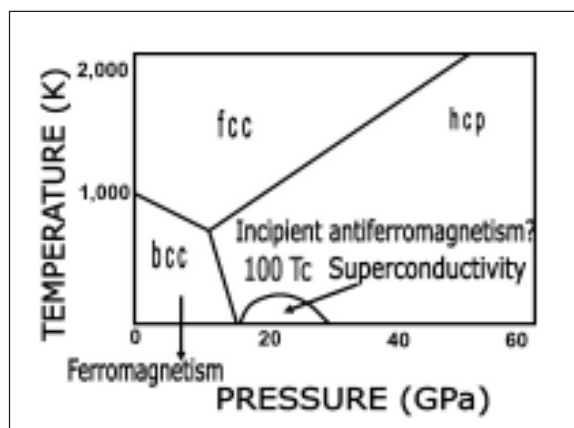


Figure 19. The phase diagram of Fe showing the superconducting phase between 15–30 GPa. In the figure, the T_c has been amplified by 100 times to see it clearly.

(Reprinted with permission from Macmillan Publishers Ltd.: *Nature*, S S Saxena and P B Littlewood, Vol.412, p.290, Copyright, 2001)

Postscript

In this two part article, the basics of high pressure techniques, and the effect of pressure on the behaviour of materials is discussed with suitable examples. This is to motivate researchers as well as teachers to venture into the world of high pressure physics and pursue research in this field. High pressure research is carried out in several leading laboratories and universities in India and abroad and is considered to be an important frontline area of research in physics, chemistry and materials science. It also has crucial implications in geophysics and astrophysics. High pressure methods are also used for exploring novel materials with exotic properties.

Acknowledgements

The authors thank N Subramanian for valuable suggestions, M Sekar, N R Sanjay Kumar and L Meenakshi Sundaram for their help in high pressure investigations and C S Sundar, P R Vasudev Rao and Baldev Raj for their support and encouragement.

Suggested Reading

Address for Correspondence
P Ch Sahu
Materials Science Division
Indira Gandhi Centre for
Atomic Research
Kalpakkam 603 102
Tamil Nadu, India.
Email: pcsahu@igcar.gov.in

- [1] A Jayaraman, *Rev. Mod. Phys.*, Vol.55, p.65, 1983. *Rev.Sci.Instrum.*, Vol.57, p.103, 1986.
- [2] D A Young, *Phase Diagrams of Elements*, University of Berkeley, 1991.
- [3] R J Hemley, H K Mao and V V Struzhkin, *J. Synch. Rad.*, Vol.12, pp.135–54, 2005.
- [4] N Subramanian, N V Chandra Shekar, N R Sanjay Kumar and P Ch Sahu, *Current Science*, Vol.91, p.177, 2006.
- [5] www.hpcat.aps.anl.gov – for latest high pressure investigations in front-line areas.

